Self-Consistent Stochastic Dynamics for Finite-Size Networks of Spiking Neurons

Gianni V. Vinci [1,2] Roberto Benzi [3,4] and Maurizio Mattia [1,*]

[1] *Natl. Center for Radiation Protection and Computational Physics, Istituto Superiore di Sanità, 00161 Roma, Italy*
[2] *PhD Program in Physics, Dept. of Physics, "Tor Vergata" University of Rome, 00133 Roma, Italy*
[3] *Dept. of Physics and INFN, "Tor Vergata" University of Rome, 00133 Roma, Italy*
[4] *Centro Ricerche "E. Fermi," 00184, Roma, Italy*

Despite the huge number of neurons composing a brain network, ongoing activity of local cell assemblies is intrinsically stochastic. Fluctuations in their instantaneous rate of spike firing $\nu(t)$ scale with the size of the assembly and persist in isolated networks, i.e., in the absence of external sources of noise. Although deterministic chaos due to the quenched disorder of the synaptic couplings underlies this seemingly stochastic dynamics, an effective theory for the network dynamics of a finite assembly of spiking neurons is lacking. Here, we fill this gap by extending the so-called population density approach including an activity- and size-dependent stochastic source in the Fokker-Planck equation for the membrane potential density. The finite-size noise embedded in this stochastic partial derivative equation is analytically characterized leading to a self-consistent and nonperturbative description of $\nu(t)$ valid for a wide class of spiking neuron networks. Power spectra of $\nu(t)$ are found in excellent agreement with those from detailed simulations both in the linear regime and across a synchronization phase transition, when a size-dependent smearing of the critical dynamics emerges.

Complex systems in statistical physics usually deal with a huge number N of interacting bodies like molecules leading to having wide applicability of effective mean-field theories. However, the finite size (e.g., volume) of the system can have a significant impact in the emergent collective dynamics [1]. This can be due to the fact that finite systems have surfaces and volumes affecting the system behavior when, for instance, phase transitions are approached [2,3]. In many cases the presence of a finite number of elements can be incorporated as a stochastic field whose fluctuation size depends on N [4,5]. In this way, the continuum formalism valid in the thermodynamic limit may result in being effective in describing small-scale phenomena across phase transitions [6]. Biological and ecological systems can be even more challenging as they may incorporate peculiar boundary conditions and heterogeneity in space and time posing them continuously outside equilibrium [7,8]. This is the case of biological networks of neurons. Here the probability current (see below) does not vanish even under stationary conditions when it matches the frequency of spikes emitted per neuron, i.e., the firing rate ν [9–12]. In this Letter, we will show that finite-size fluctuations can be effectively taken into account in this challenging system. This is done via a self-consistent definition of the noise to be embedded into the mean-field population dynamics.

Population density and mean-field approximation.—In the thermodynamic limit ($N \to \infty$) networks of single-compartment spiking neurons have collective dynamics statistically described by the probability density $p(v, t)$ of realizations with membrane potential v at time t [10–13], obeying the Fokker-Planck equation

$$\partial_t p(v, t) = -\partial_v S_p(v, t) + \delta(v - v_{\text{res}})\nu(t). \quad (1)$$

In this continuity equation the density p changes according to the divergence of the probability current $S_p = (F + \mu)p - \frac{1}{2}\partial_v(\sigma^2 p)$ and to the source of realizations reentering in the reset potential v_{res} after emitting a spike by crossing the emission threshold v_{thr}. This flux of neurons is the firing rate $\nu(t) = S_p(v_{\text{thr}}, t)$. Here, the membrane potential $V(t)$ of a single neuron follows the Langevin equation

$$dV = [F(V) + \mu(V, t)]dt + \sigma(V, t)dW, \quad (2)$$

where $F(V)$ is the drifting current determining the model-specific relaxation dynamics. In what follows, we adopt the "leaky" integrate-and-fire (LIF) neuron with $F(V) = -V/\tau$ and decay time τ as the workbench [14]. The total synaptic and ionotropic input current is a Gaussian white noise $dW(t)$ with zero mean and $\langle dW(t)dW(t')\rangle = \delta(t - t')dt$ inhomogeneously modulated in time to have infinitesimal mean $\mu(V, t)$ and variance $\sigma^2(V, t)$. In "current-based" LIF neurons, both moments are independent from V. Such diffusion approximation of the current holds in the limit of large number K of presynaptic contacts and small average synaptic efficacy J [15,16]. This is the case of cortical

networks where $K \sim 10^4$ and $J \ll v_{\text{thr}}$ [17,18]. No assumptions are made neither on the statistics of single-neuron spike trains, nor on the stationarity of the moments μ and σ^2. This because synaptic currents result from a superposition of a large number K of uniformly sparse point processes (i.e., the spike trains of presynaptic neurons), which eventually converges to a inhomogeneous Poisson process [19,20]. In the diffusion limit this process is approximated by the above Gaussian noise valid also far from equilibrium.

In this framework also the mean-field approximation holds such that all neurons of a homogeneous network can be seen as independent realizations of the same stochastic process (same F, μ, and σ) [21]. Synaptic interactions are incorporated in the ν-dependent moments of the current, which in current-based models like LIF neurons are

$$\mu(\nu) = KJ\nu(t) + \mu_{\text{ext}}$$
$$\sigma^2(\nu) = KJ^2\nu(t) + \sigma_{\text{ext}}^2. \qquad (3)$$

Here, μ_{ext} and σ_{ext}^2 are the moments of the synaptic current due to the spikes incoming from neurons external to the network. Here we impose them to be constant.

Why are finite-size fluctuations important?—Having a finite number N of neurons emitting spike trains $S_i(t) = \sum_k \delta(t - t_{i,k})$, leads to a fluctuating rate $\nu_N(t) = \sum_{i=1}^{N} S_i(t)/N = \mathcal{N}(t)$ of action potentials fired per unit time and per neuron. According to the mentioned limit theorem [19], $\mathcal{N}(t)$ is an inhomogeneous Poisson process with mean $N\nu(t)$, such that $\lim_{N\to\infty} \nu_N(t) = \nu(t)$. Mean and variance of ν_N are ν and ν/N, respectively. For large enough N (~ 100) like those observed in cortical minicolumns [22], holds the Gaussian approximation

$$\nu_N(t) = \nu(t) + \sqrt{\frac{\nu(t)}{N}}\Gamma(t) \equiv \nu(t) + \eta(t). \qquad (4)$$

Here, the finite-size noise $\eta(t)$ results from a modulation of a white noise $\Gamma(t)$ independent from $dW(t)$ in Eq. (2). The correlation structure of η will be self-consistently derived in the following. Taking into account the fluctuating ν_N into Eq. (3), the moments of the input current (i.e., the mean-field) are no longer deterministic [11]. Fluctuations of the mean μ have relative size $\text{Var}[\mu(\nu_N)]^{1/2}/\text{E}[\mu(\nu_N)] = 1/\sqrt{N\nu}$ of about 10% in cortical networks of interest where $\nu \sim 1$ Hz [23]. Remarkably, such variability is of the same order of the changes in μ associated with the coding of sensorial stimuli [24] or other relevant information [25]. Indeed, this process usually involves only a sparse set of tuned neurons with variations of few Hz in their firing rates. Thus, finite-size fluctuations may have a not negligible impact disturbing or nonlinearly amplifying the encoding dynamics of cortical networks.

How can finite-size fluctuations be incorporated?—To understand the impact of such fluctuations, according to [11] we incorporate the stochastic moments $\mu_N \equiv \mu(\nu_N)$ and $\sigma_N \equiv \sigma(\nu_N)$ directly into Eq. (1). The resulting stochastic Fokker-Planck equation describes now an infinite set of independent neurons all driven by the same fluctuating mean-field. Differently from other stochastic Smoluchowski equations [4,5] and their coarse-grained versions [26,27], here stochasticity appears as an additional probability current with drift and diffusion coefficients differently affected by $\eta(t)$. Not only, this additional source of noise must be incorporated as a fluctuating source of realizations in v_{res} [28]. This is due to the fact that the finite flux of neurons crossing the threshold v_{thr} reenters at the reset potential, eventually leading to

$$\partial_t p = -\partial_v[(F + \mu_N)p] + \frac{1}{2}\partial_v^2(\sigma_N^2 p)$$
$$+ \delta(v - v_{\text{res}})\nu_N(t). \qquad (5)$$

We remark that this stochastic Fokker-Planck (SFP) equation is nonlinear as both μ_N and σ_N depend on the density p via the firing rate ν.

Self-consistent derivation of $\eta(t)$.—To determine the statistical features of $\eta(t)$ we refer to the specific case of a set of N uncoupled neurons ($J = 0$) driven by a stationary external input ($\dot{\mu}_{\text{ext}} = \dot{\sigma}_{\text{ext}} = 0$). In this case neurons are renewal processes, and the probability density $\rho(t)$ of their interspike intervals (ISI) fully characterize the statistics of the spike trains they emit [29]. Pooling together these spike trains gives $\nu_N(t)$ (see above) such that its power spectral density is [14,30]

$$P_\nu^{(\text{RT})}(\omega) = |\hat{\nu}_N(\omega)|^2 = \frac{\nu_0}{N}\text{Re}\left[\frac{1 + \hat{\rho}(\omega)}{1 - \hat{\rho}(\omega)}\right]. \qquad (6)$$

Here $\hat{\rho}(\omega) = \int_{-\infty}^{\infty} \rho(t)e^{-i\omega t}dt$ and $\hat{\nu}_N(\omega)$ are the Fourier transform of $\rho(t)$ and $\nu_N(t)$, respectively, and $\nu_0 = 1/\int_0^\infty t\rho(t)dt$ is the mean firing rate, i.e., the inverse of the mean ISI.

This exact result must be also obtained from Eq. (5). To carry out the power spectral density $|\hat{\nu}_N(\omega)|^2$ in this case we resort to the spectral expansion approach introduced in [28] giving

$$P_\nu^{(\text{SE})}(\omega) = |1 + \vec{f} \cdot (i\omega\mathbf{I} - \mathbf{\Lambda})^{-1}\vec{\psi}_{\text{res}}|^2 |\hat{\eta}(\omega)|^2 \qquad (7)$$

(see the Appendix A). If the finite-size noise is assumed to be white, $|\hat{\eta}(\omega)|^2 = \nu_0/N$, it leads to an overestimate of the power spectral density at relatively low-ω at least under the "suprathreshold" regime, i.e., when neurons emit spikes even if $\sigma = 0$ [28].

In Eq. (7) we use the eigenfunctions $\phi_n(v)$ of the non-Hermitian Fokker-Planck operator $\mathcal{L}$ defined from Eq. (1) as $\partial_t p \equiv \mathcal{L}p$. This operator has an infinite spectrum of discrete eigenvalues λ_n ($n \in \mathbb{I}$) such that $\mathcal{L}\phi_n = \lambda_n\phi_n$

[10,13,28]. The flux $f_n = 1/2\partial_v(\sigma\phi_n)|_{v=v_{\text{thr}}}$ of nonstationary ($n \neq 0$) eigenfunctions are the infinite elements of $\vec{f}$ set to $1/\tau$ [31]. The matrix $\mathbf{\Lambda}$ is diagonal with $\{\mathbf{\Lambda}\}_{nn} = \lambda_n$. The elements of $\vec{\psi}_{\text{res}}$ are instead the eigenfunction $\psi_n(v)$ of the adjoint operator $\mathcal{L}^{\dagger}$ with same λ_n, computed in $v = v_{\text{res}}$ [13,28]. Note that all these coefficients are state dependent, being functions of the current moments μ and σ.

In this framework, the crucial observation is that for any IF neuron model, the series in Eq. (7) can be summed as a function of $\hat{\rho}(\omega)$ [32]:

$$\vec{f} \cdot (i\omega\mathbf{I} - \mathbf{\Lambda})^{-1}\vec{\psi}_{\text{res}} = \frac{\hat{\rho}(\omega)}{1 - \hat{\rho}(\omega)} - \frac{\nu_0}{i\omega} \qquad (8)$$

(see the Appendix B). Using it in Eq. (7) and requiring the equivalence $P_\nu^{(\text{SE})}(\omega) = P_\nu^{(\text{RT})}(\omega)$, we obtain with Eq. (6) a self-consistent expression for the power spectrum of η:

$$|\hat{\eta}(\omega)|^2 = \frac{\nu_0}{N}\left[1 - \left|\frac{(i\omega + \nu_0)\hat{\rho}(\omega) - \nu_0}{\nu_0\hat{\rho}(\omega) + i\omega - \nu_0}\right|^2\right]. \qquad (9)$$

This equation is one of the main results of this Letter. In the limit $\omega \to \infty$, $\hat{\rho}(\omega) \to 0$ and the finite-size noise is white-like with variance ν_0/N. For $\omega \to 0$, the lhs of Eq. (8) reduces to $-\vec{f} \cdot \mathbf{\Lambda}^{-1}\vec{\psi}_{\text{res}} = (c_v^2 - 1)/2$ [32], the function of the coefficient of variation c_v of the ISIs, leading to

$$|\hat{\eta}(0)|^2 = \frac{\nu_0}{N}\frac{4c_v^2}{(1 + c_v^2)^2}. \qquad (10)$$

These limits suggest a sigmoidlike power spectra of the finite-size noise which is confirmed in LIF neurons [Fig. 1(a)]. For this type of neuron models $\hat{\rho}(\omega) = \sqrt{e^{x_r^2 - x_t^2}}\mathcal{D}_{-i\omega}(-\sqrt{2}x_r)/\mathcal{D}_{-i\omega}(-\sqrt{2}x_t)$ with $\mathcal{D}_\nu(z)$ the parabolic cylinder function, $x_t = (v_{\text{thr}} - \mu\tau)/\sigma\sqrt{\tau}$ and $x_r = (v_{\text{res}} - \mu\tau)/\sigma\sqrt{\tau}$ [33]. As the firing regimes moves from noise- to drift-dominated (i.e., from sub- to suprathreshold) regimes by increasing the mean current μ, the sigmoidal shape becomes increasingly more apparent. Indeed, ISIs are more and more regular leading to a decrease of their c_v, and hence to a lower power $|\hat{\eta}(0)|^2$.

Markovian embedding of $\eta(t)$.—Having derived in Eq. (9) the correlation structure of the finite-size noise for a set of uncoupled neurons under stationary condition a question arises: can we generalize this result to networks of synaptically coupled neurons and far from equilibrium?

To answer this question we remark that the spectra from Eq. (9) shown in Fig. 1 are flat (white noiselike) with a power reduction at low-ω possibly resulting by subtracting a Lorentzian-shaped function. Following [34], such kinds of spectra are well approximated by two-dimensional Ornstein-Uhlenbeck processes $\vec{u}(t)$ driven by and interfering with the same white noise $\Gamma(t)$:
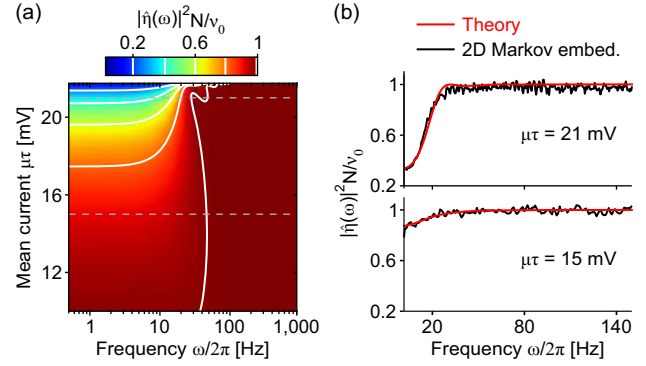

FIG. 1. Normalized power spectra of the finite-size noise η for N uncoupled LIF neurons with firing rate ν_0. (a) $|\hat{\eta}(\omega)|^2 N/\nu_0$ as a function of the mean synaptic current μ. σ is chosen to keep the mean firing rate unchanged at $\nu_0 = 20$ Hz. (b) In noise-dominate regime ($\mu\tau < v_{\text{thr}} = 20$ mV) finite-size noise is essentially white (bottom). In drift-dominate regime, power is low at low-ω as ISIs are more regular ($c_v < 1$). In both cases, a two-dimensional Markovian embedding (black) faithfully reproduce theoretical spectra (red) from Eq. (9).

$$d\vec{u} = \mathbf{A}\vec{u}dt + \vec{b}\Gamma dt^{1/2}$$

$$\eta = \vec{1} \cdot \vec{u} + \sqrt{\frac{\nu}{N}}\Gamma. \qquad (11)$$

In Fig. 1(b) we show that for $\nu(t) = \nu_0$ this Markovian embedding faithfully reproduces the correlation structure of $\eta(t)$ in the simple case of $\vec{b}$ with only one nonzero element, $b_1 = \sqrt{\nu/N}$, and of a three-parameter $\mathbf{A}$ being $A_{11} = A_{22}$. Instead of fitting $\{A_{11}, A_{12}, A_{21}\}$, we carry them out analytically as in [34] by matching the power of η from Eq. (11) with the exact one in Eq. (9) at the frequencies: $\omega = \{0, \pi, 2\pi\}\nu_0$. The parameters change according to μ and σ leading to a state-dependent $\mathbf{A}(\mu, \sigma)$.

This dynamical description of $\eta(t)$ in principle allows us to overcome the renewal hypothesis. Indeed, here the memory embedded in the network activity is reintroduced via the dependence on $\nu(t)$ of the current moments in Eq. (3). We then conjecture that Eqs. (4), (5), and (11) provide a complete statistical description of the out-of-equilibrium dynamics of finite-size networks of spiking neurons, thus positively answering to the above question.

Effectiveness of the stochastic network dynamics.—To test this conjecture, we use a network of excitatory LIF neurons with a distribution of transmission delays of the emitted spikes. In the limit $N \to \infty$, the chosen network displays a supercritical Hopf bifurcation as coupling KJ increases. Here a limit cycle arises through the destabilization of an equilibrium point with firing rate $\nu_0 = 20$ Hz (see the Appendix D).

In weakly coupled networks with relatively small KJ, finite-size noise induces stochastic perturbations of $\nu_N(t)$ around a stable focus amenable to linear response theory.
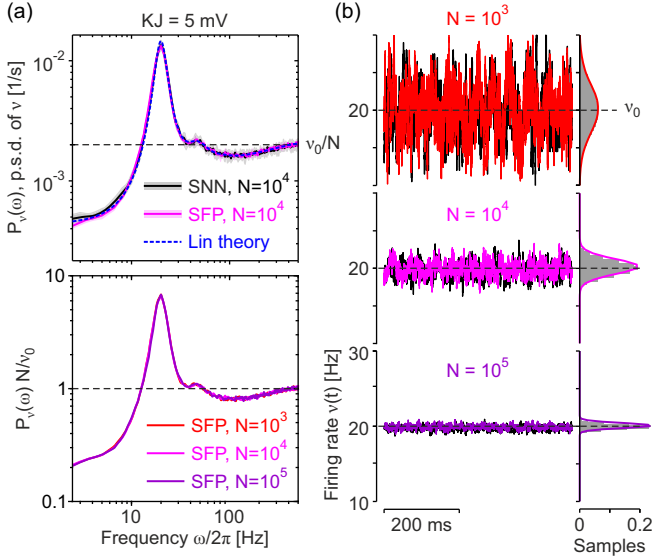
FIG. 2. Power spectra $P_\nu(\omega)$ (a) and firing rates $\nu_N(t)$ (b) of weakly coupled networks ($KJ = 5$ mV) with varying size N. (a) Top, $P_\nu(\omega)$ from the numerical integration of the stochastic Fokker-Planck equation (SFP, pink), the equivalent spiking neuron network (SNN) simulation (black) and linear perturbation theory [dashed blue from Eq. (12)] ($N = 10^4$). Dashed black, white noise with variance ν_0/N. Bottom, normalized spectra of ν from SFP of networks with different N ($= 10^3, 10^4, 10^5$). (b) $\nu_N(t)$ from SNN simulations (black) and SFP varying N ($= 10^3, 10^4, 10^5$) (left). Right, related histograms of $\nu_N(t)$. Other parameters as in Fig. 4.

This is the case of our example network with $KJ = 5$ mV for which the power spectrum of ν_N can be carried out as a linear transformation of the finite-size noise [28,35]:

$$P_\nu(\omega) = |\hat{\nu}_N(\omega)|^2 = |\hat{H}_\nu(\omega)|^2 |\hat{\eta}(\omega)|^2. \quad (12)$$
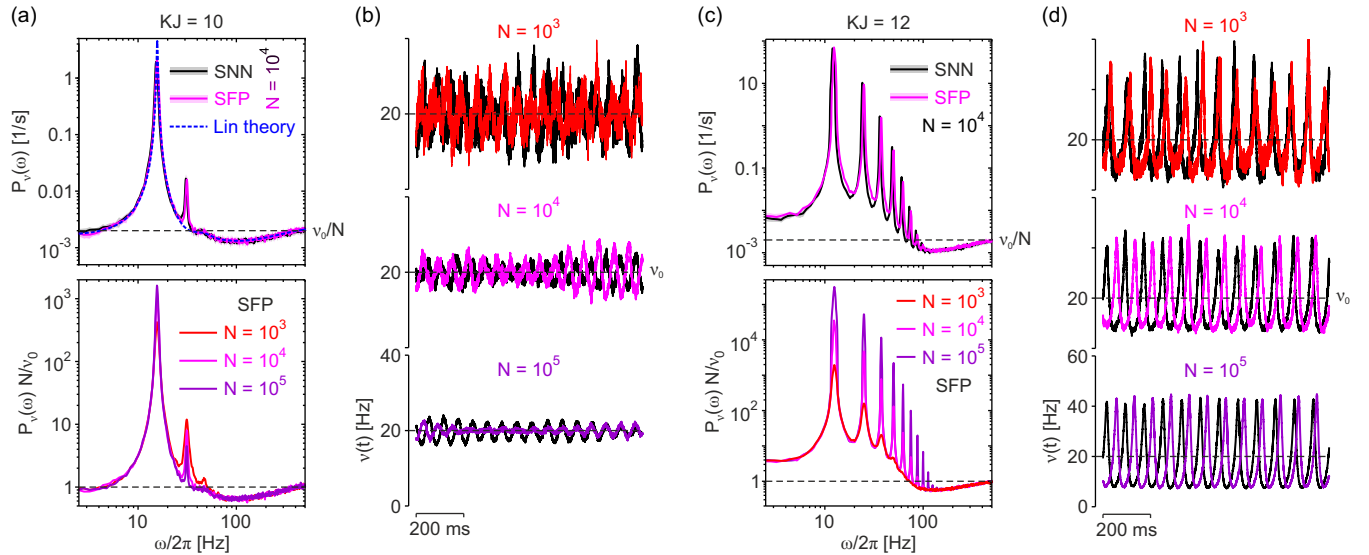
Here $\hat{H}_\nu(\omega)$ is the Fourier transfer function characterizing the linear response to sinusoidal modulations of the input firing. $\hat{H}_\nu(\omega)$ is analytically known for LIF neurons [11,36]. In Fig. 2(a), top we show a remarkable agreement between such Eq. (12) and the power spectral densities $P_\nu(\omega)$ estimated from both the simulations of spiking neuron networks (SNN [37]) and the numerical integration of the SFP Eq. (5). To compute the SFP integration we extended a standard deterministic approach [38] by incorporating the Markovian embedding (11) of $\eta(t)$ (see the Appendix C). SFP integration for different network sizes N confirms in Fig. 2(a), bottom what was expected from the linear theory, that is, the spectrum shape does not change with N once normalized by the variance ν_0/N. The equivalence in these cases between SNN simulation and SFP integration is also apparent in the direct comparison of $\nu_N(t)$ time series. Indeed, in Fig. 2(b) no differences emerge and both time series display a variance scaling as $1/N$, as expected.

By further increasing the synaptic coupling KJ, the mentioned Hopf bifurcation is approached (Fig. 4 in Appendix D) and finite-size networks have $P_\nu(\omega)$ no longer fully described by linear theory [i.e., Eq. (12)]. The mismatch is apparent in Fig. 3(a), top as an unpredicted second-harmonic peak at $\omega/2\pi \simeq 2\nu_0$ arises in SNN simulations. On the contrary, the SFP integration displays an excellent match. Despite such a footprint of nonlinear dynamics, SNN and SFP keep displaying a remarkable overlap not only in P_ν but also in the stochastic dynamics of $\nu_N(t)$ shown in Fig. 3(b). There coherent oscillations become more and more apparent as N decreases. In this case ongoing finite-size fluctuations of ν_N continuously stimulate the oscillating relaxation of the stable focus

FIG. 3. Power spectra $P_\nu(\omega)$ (a),(c) and firing rates $\nu_N(t)$ (b),(d) of strongly coupled (nonlinear) networks with varying size N. (a), (b) $KJ = 10$ mV, mean-field dynamics predicts a stable focus at $\nu_0 = 20$ Hz. (c),(d) $KJ = 12$ mV, networks beyond a supercritical Hopf bifurcation with a stable limit cycle. See Figs. 2 and 4 for additional details.

which is relatively slow due to the nearby critical point [see Fig. 4(b), middle]. The N-dependent coherence of the fluctuation-driven oscillations is even more apparent in the increase of power of the second-harmonic peak in smaller networks [Fig. 3(a), bottom].

The same remarkable match between SFP and SNN is shown in Fig. 3(c), top beyond the Hopf bifurcation ($KJ = 12$ mV) when a stable limit cycle is expected at $N \to \infty$. Global oscillations in this case are strongly nonlinear, giving rise to several high-order harmonic peaks. In this case finite-size noise contributes to dephase the oscillations limiting their coherence in time [Fig. 3(d)]. According to this, the resonant peaks in $P_\nu(\omega)$ have power lowering with decreasing N [Fig. 3(c), bottom].

Conclusions.—The agreement between SFP and SNN in a synchronization phase transition proves that the stochastic dynamics derived in Eqs. (4), (5), and (11) can faithfully describe finite networks of spiking neurons far from equilibrium. Indeed, the theoretical framework we introduce is not perturbative and takes into account the pointlike (spike-based) nature of the cell-to-cell interactions. Remarkably, the correlation structure of $\eta(t)$ here results from the spiking statistics of isolated neurons, implying that finite-size noise is not J dependent.

As the self-consistent derivation of $\hat{\eta}(\omega)$ in Eq. (9) is exact, it is valid for any N and hence also for extremely small networks. However, in addition to this "nonperturbative cornerstone" of our approach, we assume that $\eta(t)$ is generated by the embedding in Eq. (11). In doing so, we approximate $\nu_N(t)$ to a Gaussian process in Eq. (4). It implies that the number of spikes emitted by the network on its characteristic timescale τ is large ($N \gg 1/\nu\tau$). If this is not the case, the Gaussian $\nu_N(t)$ has a not negligible likelihood to be negative, thus posing a lower bound to the minimum N we can describe.

Finite-size fluctuations can elicit coherent oscillations even when equilibrium points are stable at $N \to \infty$. The size of the network is then a structural feature capable of amplifying an otherwise damped rhythmic activity. As a result, a second-harmonic peak in the power spectrum of the neuronal activity arises even without crossing a critical point. In brain networks of behaving animals, this kind of resonant peak has been observed both during sensory processing [39] and in working memory tasks [40]. Coherent rhythms across networks are supposed to make information transmission effective [41] and to facilitate the coordination underpinning several cognitive functions [42]. Oscillations induced by finite-size fluctuations can then make available a cognitive-relevant substrate without inducing a phase transition in the network.

Alternative approaches dealing with finite-size networks of spiking neurons are those relying on the refractory density method (RDM) [43]. Neurons in this case are quasistationary renewal processes and the population dynamics is fully described by the probability density of a single cell to be into a refractory state [44,45]. In the

RDM, the integro-differential equation governing the population activity at the mesoscopic scale can incorporate fluctuations to describe a finite number of neurons [46,47]. However, the quasistationarity hypothesis underlying RDM may in principle limit its applicability by making our theoretical framework preferable in dealing with out-of-equilibrium conditions.

In conclusion, we remark that our theoretical framework applies to a wide class of spiking neuron models, and it can be extended to other systems with a finite size. Indeed, including fluctuations in population density theories can further advance our understanding of noise-driven out-of-equilibrium dynamics [6,48]. An example is the metastable dynamics driven by the rotational components arising from the broken detailed balance in biological systems [49,50].

Appendix A: Spectral expansion and power spectrum of ν.—Following [28], the SFP Eq. (5) can be rewritten as an infinite set of differential equations for the projection coefficients $a_n(t) = \int_{-\infty}^{v_{thr}} \psi_n(v)p(v, t)dv$ of p onto the eigenfunctions $\psi_n(v)$. Briefly, this can be done by applying $\int_{-\infty}^{v_{thr}} dv \psi_n(v)$ to both sides of Eq. (5), eventually obtaining the stochastic firing rate equation

$$\dot{\vec{a}} = (\mathbf{\Lambda} + \mathbf{C}\dot{\nu}_N)\vec{a} + \vec{c}\dot{\nu}_N + \vec{\psi}_{res}\eta$$
$$\nu_N = \Phi + \vec{f} \cdot \vec{a} + \eta. \tag{A1}$$

For the sake of simplicity, we resorted to a matrix formalism where $\{\vec{a}\}_n = a_n(t)$, and the "coupling" coefficients $c_{nm} = \int_{-\infty}^{v_{thr}} \phi_m(v)\partial_\nu \psi_n(v)dv$ compose the infinite vector $\{\vec{c}\}_n = c_{n0}$ and matrix $\{\mathbf{C}\}_{nm} = c_{nm}$, given n, $m \neq 0$. The coupling label comes from the fact that these coefficients directly depend on the synaptic efficacy J as, from Eq. (3), $\partial_\nu = \partial_\nu \mu \partial_\mu + \partial_\nu \sigma^2 \partial_{\sigma^2} \sim J$. Here, the "stationary mode" ($n = 0$) with $\lambda_0 = 0$ and probability density $\phi_0(v)$ has been isolated, and it gives the current-to-rate gain function $\Phi(\mu, \sigma^2) \equiv f_0$, i.e., the stationary firing rate ν_0 of the network (see, for instance, [14]). Other definitions are as in the main text.

Under stationary conditions ($\dot{\mu}_{ext} = 0$ and $\dot{\sigma}_{ext} = 0$), the firing rate equation (A1) for a set of uncoupled neurons ($\vec{c} = 0$ and $\mathbf{C} = 0$ being $J = 0$) reduces to

$$\dot{\vec{a}} = \mathbf{\Lambda}\vec{a} + \vec{\psi}_{res}\eta$$
$$\nu_N = \Phi + \vec{f} \cdot \vec{a} + \eta, \tag{A2}$$

where all the coefficients are now constant. The Fourier transform of the firing rate is then $\hat{\nu}_N(\omega) = \vec{f} \cdot \hat{\vec{a}}(\omega) + \hat{\eta}(\omega)$, where $\hat{\vec{a}}(\omega) = (i\omega\mathbf{I} - \mathbf{\Lambda})^{-1}\vec{\psi}_{res}\hat{\eta}(\omega)$. Given that, an

explicit expression $P_\nu^{(SE)}(\omega) = |\hat{\nu}_N(\omega)|^2$ can be worked out leading to Eq. (7).

Appendix B: ISI density ρ and relaxation dynamics of ν.—To establish the relationship between the probability density $\rho(t)$ of the ISIs and the relaxation dynamics of an uncoupled set of neurons we follow [32]. Briefly, for renewal point processes like LIF neurons with initial condition $V(0) = v_{res}$, the density $\nu(t)$ of spikes emitted per unit time has Laplace transform $\hat{\nu}(s) = \int_0^\infty e^{-st}\nu(t)dt$ given by [14,16]

$$\hat{\nu}(s) = \frac{\hat{\rho}(s)}{1 - \hat{\rho}(s)}, \tag{B1}$$

where $\hat{\rho}(s)$ is the Laplace transform of $\rho(t)$. Here, the firing rate $\nu(t)$ can be obtained from Eq. (A2) in the limit $N \to \infty$ ($\eta \to 0$ such that $\nu_N \to \nu$):

$$\dot{\vec{a}} = \boldsymbol{\Lambda}\vec{a}$$
$$\nu = \nu_0 + \vec{f} \cdot \vec{a}. \tag{B2}$$

Applying the operator $\int_0^\infty dt e^{-st}$ to both sides of this system we obtain the following expression

$$s\hat{\vec{a}}(s) - \vec{a}(0) = \boldsymbol{\Lambda}\hat{\vec{a}}(s)$$
$$\hat{\nu}(s) = \frac{\nu_0}{s} + \vec{f} \cdot \hat{\vec{a}}(s),$$

yielding the Laplace transform $\hat{\vec{a}}(s) = (s\mathbf{I} - \boldsymbol{\Lambda})^{-1}\vec{a}(0)$. For the mentioned initial conditions, i.e., $p(v,0) = \delta(v - v_{res})$, the projection coefficients at $t = 0$ result to be $\{\vec{a}(0)\}_n = \int_{-\infty}^{v_{thr}} \psi_n(v)\delta(v - v_{res})dv = \psi_n(v_{res}) \equiv \{\vec{\psi}_{res}\}_n$. Putting together these results allows us to write

$$\hat{\nu}(s) = \frac{\nu_0}{s} + \vec{f} \cdot (s\mathbf{I} - \boldsymbol{\Lambda})^{-1}\vec{\psi}_{res}, \tag{B3}$$

which, once compared with Eq. (B1), proves Eq. (8) provided that we move from the Laplace to the Fourier transform by setting $s = i\omega$.

Appendix C: Numerical analysis.—The continuity equation (1) is a nonlinear PDE with the following boundary conditions: (i) neurons emitting a spike cross an absorbing barrier in $v = v_{thr}$, $p(v_{thr}) = 0$; (ii) after a refractory period τ_0 from spike emission, neurons reenter in $v = v_{res}$ requiring the conservation of the probability current, $S_p(v_{thr}, t - \tau_0) = S_p(v_{res}^+, t) - S_p(v_{res}^-, t)$; and (iii) membrane potential is limited to $v \geq v_{min}$ by setting a reflecting barrier, $S_p(v_{min}) = 0$. For the sake of simplicity, here $\tau_0 = 0$ and $v_{min} \to -\infty$. To numerically integrate Eq. (1), we resorted to the open-source software described in [38]. It implements a voltage and time discretization scheme based on the Scharfetter-Gummel flux [51] and taking into account the above boundary conditions. We adapted this software by

incorporating finite-size fluctuations to integrate the SFP Eq. (5) [52]. Briefly, at each time step dt the firing rate $\nu_N(t)$ of a network composed of N neurons is computed by adding the finite-size noise $\eta(t)$ to the flux $\nu(t) = S_p(v_{thr})$. The noise $\eta(t)$ is worked out resorting to the Euler-Maruyama method to integrate the Itô defined Eq. (11) [53].

In the SFP Eq. (5), we consider the moments of the synaptic current Eq. (3) being dependent on the rate of incoming spikes $K\tilde{\nu}(t)$ instead of $K\nu_N(t)$. This is because the example networks in Figs. 2 and 3 incorporate a distribution $g(\delta)$ of axonal delays δ such that

$$\tilde{\nu}(t) = \int_0^\infty g(\delta)\nu_N(t - \delta)d\delta, \tag{C1}$$

where $g(\delta) = e^{-(\delta - \delta_{min})/\tau_\delta}/\tau_\delta$ vanishing for any $\delta < \delta_{min}$, and with mean delay $\langle \delta \rangle = \tau_\delta + \delta_{min}$. For the numerical integration we resorted to the equivalent expression $\tau_\delta\dot{\tilde{\nu}}(t) = \nu_N(t - \delta_{min}) - \tilde{\nu}(t)$ [28,54]. The reentering flux in v_{res} of realizations or neurons just having emitted a spike, is taken into account by setting at each time step $S_p(v_{res}^+, t) - S_p(v_{res}^-, t) = \nu_N(t)$.

Spiking neuron networks were simulated resorting to the open source NEST simulator [37]. Network and neuron parameters are those detailed in Fig. 4. Further details can
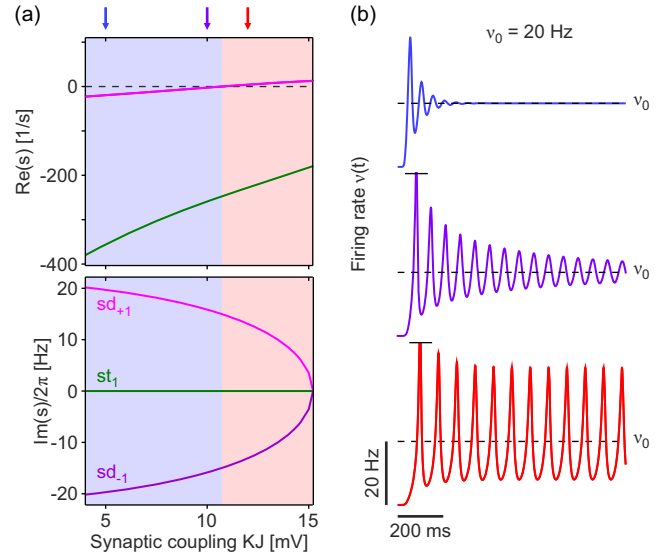

FIG. 4. Bifurcation analysis of the network of LIF excitatory neurons ($N \to \infty$) studied in Figs. 2 and 3 at varying synaptic efficacies J. (a) Real and imaginary parts of the poles $sd_{\pm 1}$ and st_1 of $\nu(s)$ solving Eq. (D2). Weakly coupled networks (small KJ, blue range) have a stable focus in ν_0. Beyond $KJ \simeq 11$ mV (red) limit cycles arise *via* a codimension-1 supercritical Hopf bifurcation. (b) Numerical integration of the Fokker-Planck equation with $p(v,0) = \delta(v - v_{res})$ for $KJ = \{5, 10, 12\}$ mV pointed out in (a) (top arrows). The fixed point at $\nu_0 = 20$ Hz is kept constant by setting $\mu\tau = 21$ and $\sigma\tau^{1/2} = 2.665$ mV, and changing μ_{ext} and σ_{ext} according to J. Other parameters: $K = 10^3$, $\tau = 20$ ms, $v_{thr} = 20$ mV, $\delta_{min} = 2$ ms, and $\tau_\delta = 1$ ms.

be found in the freely available PYTHON scripts we developed [52].

Appendix D: The example network and its linear stability.—As a case study (Figs. 2 and 3) we used a network of LIF excitatory neurons, which in the thermodynamic limit ($N \to \infty$) has an equilibrium point with $\nu_0 = 20$ Hz, Fig. 4.

In the network the spikes are exchanged with the distribution of axonal delays δ defined in Eq. (C1). Delayed couplings in an excitatory network can give rise to limit cycles, making it an ideal workbench to test our theoretical framework. We then focus on a codimension-1 Hopf bifurcation by changing the synaptic efficacy $J > 0$ and keeping fixed the firing rate $\nu_0 = \Phi(\mu, \sigma)$. That is done by imposing constant moments $\mu(\nu_0)\tau = 21$ and $\sigma(\nu_0)\sqrt{\tau} = 2.665$ mV. According to Eq. (3), it requires then to vary both μ_{ext} and σ_{ext} as a function J.

Following [28], the stability of the equilibrium point is evaluated by linearizing Eq. (A1) in the limit $N \to \infty$ ($\eta \to 0$). To this purpose we set $\nu(t) \simeq \nu_0 + \nu_1(t)$ with $\nu_1(t) = \mathcal{O}(|\vec{a}|)$ and neglect higher-order terms $\mathcal{O}(|\vec{a}|^2)$. The firing rate equation then reduces to

$$\dot{\vec{a}} = \mathbf{\Lambda}\vec{a} + \vec{c}\dot{\tilde{\nu}}_1$$
$$\nu_1 = \Phi'\tilde{\nu}_1 + \vec{f} \cdot \vec{a}, \tag{D1}$$

where all coefficients and eigenvalues are now computed in $\nu = \nu_0$, $\Phi' = \partial_\nu\Phi|_{\nu=\nu_0}$, and $\tau_\delta\dot{\tilde{\nu}}_1 = \nu(t - \delta_{\text{min}}) - \tilde{\nu}(t) = \nu_1(t - \delta_{\text{min}}) - \tilde{\nu}_1(t)$ to take into account the distribution of delays δ. As done above for Eq. (B2), the Laplace transform of the firing-rate perturbation $\hat{\nu}_1(s)$ can be worked out given that $\hat{\tilde{\nu}}_1(s) = \hat{\nu}_1(s)e^{-s\delta_{\text{min}}}/(1 + s\tau_\delta) = \hat{\nu}_1(s)\hat{g}(s)$. The poles of $\hat{\nu}_1(s)$ determine the stability of the equilibrium point. Once $\hat{\nu}_1(s)$ is made explicit, the poles are the zeros of its denominator:

$$1 - \hat{g}(s)[\Phi' + s\vec{f}(s\mathbf{I} - \mathbf{\Lambda})^{-1}\vec{c}] = 0. \tag{D2}$$

As shown in [28], these zeros are well approximated by taking into account only the two leading eigenmodes [i.e., with smallest $-\text{Re}(\lambda_n)$, here $n = -1, 1$], such that

$$s\vec{f}(s\mathbf{I} - \mathbf{\Lambda})^{-1}\vec{c} \simeq \frac{s}{\tau}\left(\frac{c_{+10}}{s - \lambda_{+1}} + \frac{c_{-10}}{s - \lambda_{-1}}\right). \tag{D3}$$

With this in Eq. (D2) we have a third degree equation for s with the solutions $s^* = \{\text{sd}_{\pm 1}, \text{st}_1\}$ shown in Fig. 4(a). As we set $\mu\tau > v_{\text{thr}}$, the equilibrium point ν_0 is in a supra-threshold regime and the first two eigenvalues are $\lambda_{\pm 1} \simeq -2(\pi\sigma/v_{\text{thr}})^2 \pm 2\pi\nu_0$ [10,13,28]. With this guess we compute the exact $\lambda_{\pm 1}$ by finding the numerical solution of the characteristic equation $\psi_\lambda(v_{\text{thr}}) = \psi_\lambda(v_{\text{res}})$ [13,28]. Knowing the eigenvalues, the coefficients c_{n0} for the

LIF neuron have an analytic expression in terms of parabolic cylinder functions [32]. The poles s^* are eventually computed by making use of these $\lambda_{\pm 1}$ and $c_{\pm 10}$.

In Fig. 4(a), for small enough synaptic couplings KJ, all poles have negative real parts. The equilibrium point is then a stable focus ($\text{sd}_{\pm 1}$ are complex conjugates) as shown in the two example networks with $KJ = 5$ and 10 mV [Fig. 4(b), top]. By further increasing KJ, the focus destabilizes at about 11 mV via a supercritical Hopf bifurcation giving rise to a stable limit cycle, as shown in Fig. 4(b), bottom ($KJ = 12$ mV).

---

*maurizio.mattia@iss.it

[1] N. G. van Kampen, *Stochastic Processes in Physics and Chemistry*, 3rd ed. (North Holland, Amsterdam, 2007), ISBN 9780444529657.

[2] C.-C. Chen, A. B. Herhold, C. S. Johnson, and A. P. Alivisatos, Science **276**, 398 (1997).

[3] I.-S. Hwang, S.-H. Chang, C.-K. Fang, L.-J. Chen, and T. T. Tsong, Phys. Rev. Lett. **93**, 106101 (2004).

[4] K. Kawasaki, Physica (Amsterdam) **208A**, 35 (1994).

[5] D. S. Dean, J. Phys. A: Math. Gen. **29**, L613 (1996).

[6] M. A. Durán-Olivencia, P. Yatsyshin, B. D. Goddard, and S. Kalliadasis, New J. Phys. **19**, 123022 (2017).

[7] M. Pascual and S. A. Levin, Ecology **80**, 2225 (1999).

[8] S. Gupta, A. Campa, and S. Ruffo, J. Stat. Mech. (2014) R08001.

[9] B. W. Knight, J. Gen. Physiol. **59**, 734 (1972).

[10] L. F. Abbott and C. van Vreeswijk, Phys. Rev. E **48**, 1483 (1993).

[11] N. Brunel and V. Hakim, Neural Comput. **11**, 1621 (1999).

[12] S. Fusi and M. Mattia, Neural Comput. **11**, 633 (1999).

[13] B. W. Knight, D. Manin, and L. Sirovich, in *Proceedings of the Symposium on Robotics and Cybernetics: Computational Engineering in Systems Applications*, edited by E. Gerf (Cite Scientifique, Cite Scientifique, Lille, France, 1996), pp. 1–5.

[14] W. Gerstner, W. M. Kistler, R. Naud, and L. Paninski, *Neuronal Dynamics: From Single Neurons to Networks and Models of Cognition* (Cambridge University Press, Cambridge, England, 2014).

[15] L. M. Ricciardi, Biol. Cybern. **24**, 237 (1976).

[16] H. C. Tuckwell, *Introduction to Theoretical Neurobiology: Volume 2, Nonlinear and Stochastic Theories* (Cambridge University Press, Cambridge, England, 1988), Vol. 8.

[17] J. DeFelipe, L. Alonso-Nanclares, and J. I. Arellano, J. Neurocytol. **31**, 299 (2002).

[18] H. Markram, E. Muller, S. Ramaswamy, M. W. Reimann, M. Abdellah *et al.*, Cell **163**, 456 (2015).

[19] B. Grigelionis, Theory Probab. **8**, 177 (1963).

[20] H. C. Tuckwell, *Stochastic Processes in the Neurosciences* (Society for Industrial and Applied Mathematics (SIAM), Phyladelphia, 1989), ISBN 0898712327.

[21] D. J. Amit and N. Brunel, Cereb. Cortex **7**, 237 (1997).

[22] V. B. Mountcastle, Brain **120**, 701 (1997).

[23] B. O. Watson, D. Levenstein, J. P. Greene, J. N. Gelinas, and G. Buzsáki, Neuron **90**, 839 (2016).

[24] C. Poo and J. S. Isaacson, Neuron **62**, 850 (2009).

[25] M. Rigotti, O. Barak, M. R. Warden, X.-J. Wang, N. D. Daw, E. K. Miller, and S. Fusi, Nature (London) **497,** 585 (2013).

[26] P.-H. Chavanis, Physica (Amsterdam) **387A,** 5716 (2008).

[27] P.-H. Chavanis, Entropy **17,** 3205 (2015).

[28] M. Mattia and P. Del Giudice, Phys. Rev. E **66,** 051917 (2002).

[29] D. R. Cox and H. D. Miller, *The Theory of Stochastic Processes* (CRC Press, Boca Raton, 1977), Vol. 134.

[30] B. Lindner, Phys. Rev. E **73,** 022901 (2006).

[31] T. Deniz and S. Rotter, Phys. Rev. E **95,** 012412 (2017).

[32] G. V. Vinci and M. Mattia, Zenodo (2021), 10.5281/zenodo.5519083.

[33] A. Siegert, Phys. Rev. **81,** 617 (1951).

[34] S. Vellmer and B. Lindner, Phys. Rev. Res. **1,** 023024 (2019).

[35] M. Mattia and P. Del Giudice, Phys. Rev. E **70,** 052903 (2004).

[36] B. Lindner and L. Schimansky-Geier, Phys. Rev. Lett. **86,** 2934 (2001).

[37] T. Fardet, S. B. Vennemo, J. Mitchell, H. Mørk, S. Graber, J. Hahne *et al.*, Zenodo (2020), 10.5281/zenodo.3605514.

[38] M. Augustin, J. Ladenbauer, F. Baumann, and K. Obermayer, PLoS Comput. Biol. **13,** e1005545 (2017).

[39] M. A. Gieselmann and A. Thiele, Eur. J. Neurosci. **28,** 447 (2008).

[40] B. Pesaran, J. S. Pezaris, M. Sahani, P. P. Mitra, and R. A. Andersen, Nat. Neurosci. **5,** 805 (2002).

[41] P. Fries, Neuron **88,** 220 (2015).

[42] A. K. Engel, P. Fries, and W. Singer, Nat. Rev. Neurosci. **2,** 704 (2001).

[43] T. Schwalger and A. V. Chizhov, Curr. Opin. Neurobiol. **58,** 155 (2019).

[44] W. Gerstner, Phys. Rev. E **51,** 738 (1995).

[45] W. Gerstner, Neural Comput. **12,** 43 (2000).

[46] T. Schwalger, M. Deger, and W. Gerstner, PLoS Comput. Biol. **13,** e1005507 (2017).

[47] V. Schmutz, E. Löcherbach, and T. Schwalger, arXiv:2106.14721.

[48] S. K. Das, S. Roy, S. Majumder, and S. Ahmad, Europhys. Lett. **97,** 66006 (2012).

[49] C. W. Lynn, E. J. Cornblath, L. Papadopoulos, M. A. Bertolero, and D. S. Bassett, Proc. Natl. Acad. Sci. U.S.A. **118,** e2109889118 (2021).

[50] B. A. W. Brinkman, H. Yan, A. Maffei, I. M. Park, A. Fontanini, J. Wang, and G. La Camera, Appl. Phys. Rev. **9,** 011313 (2022).

[51] D. L. Scharfetter and H. K. Gummel, IEEE Trans. Electron Devices **16,** 64 (1969).

[52] G. V. Vinci (2021), github:/giav1n/StochasticFokkerPlanck, https://github.com/giav1n/StochasticFokkerPlanck.git.

[53] H. Risken, *Fokker-Planck Equation* (Springer, New York, 1984).

[54] M. Mattia, M. Biggio, A. Galluzzi, and M. Storace, PLoS Comput. Biol. **15,** e1007404 (2019).